SIAM J. APPL. MATH.
Vol. 63, No. 2, pp. 683–707

ON A DOUBLY NONLINEAR PARABOLIC OBSTACLE PROBLEM MODELLING ICE SHEET DYNAMICS*

N. CALVO†, J. I. DÍAZ‡, J. DURANY†, E. SCHIAVI§, AND C. VÁZQUEZ¶

Abstract. This paper deals with the weak formulation of a free (moving) boundary problem arising in theoretical glaciology. Considering shallow ice sheet flow, we present the mathematical analysis and the numerical solution of the second order nonlinear degenerate parabolic equation modelling, in the isothermal case, the ice sheet non-Newtonian dynamics. An obstacle problem is then deduced and analyzed. The existence of a free boundary generated by the support of the solution is proved and its location and evolution are qualitatively described by using a comparison principle and an energy method. Then the solutions are numerically computed with a method of characteristics and a duality algorithm to deal with the resulting variational inequalities. The weak framework we introduce and its analysis (both qualitative and numerical) are not restricted to the simple physics of the ice sheet model we consider nor to the model dimension; they can be successfully applied to more realistic and sophisticated models related to other geophysical settings.

Key words. ice sheet models, nonlinear degenerate equations, free boundaries, weak solutions, finite elements, duality methods

AMS subject classifications. 35K65, 35K85, 65C20, 65N30

PII. S0036139901385345

1. Introduction.

Modelling ice sheet dynamics has been a challenging problem since the beginning of the century, but nowadays the scientific community is showing a renewed, growing interest towards this problem. In fact, our understanding of climate system dynamics depends on the comprehension and predictability of the ice sheet dynamics. Large ice sheets influence and are influenced by climate, and their oscillations may be responsible for sudden shifts in climate in the recent geological past (Fowler [30]). The study of ice sheet models (ISM) is fundamental to the construction and comprehension of global energy balance models (EBM) and general circulation models (GCM) (see, for instance, Tarasov and Peltier [38] for a coupled ISM/EBM model). Various physically based theories have appeared during the last decades in order to explain the flow of these large ice masses, but a proper mathematical treatment is not available yet. This introduces the main aim of this paper, which is to present the mathematical and numerical analysis of an obstacle problem formulation for the study of the slow, isothermal, one-dimensional flow of ice along a rigid impermeable bed. This paper is organized as follows: after a brief description of the model equation and its strong formulation (section 2), we introduce in section 3 some weak formulations that we shall use later. The well-posedness of the model is then considered. Section 4 is devoted to the (qualitative) study of the free (moving)

*Received by the editors February 16, 2001; accepted for publication (in revised form) June 4, 2002; published electronically December 19, 2002. Partially supported by Research Projects of the D.G.E.S. (REN2000-0766) and M.C.Y.T. (BFM2001-3261-C02).

http://www.siam.org/journals/siap/63-2/38534.html

†Departamento de Matemática Aplicada, E.T.S.I. de Telecomunicaciones, Universidade de Vigo, Campus Marcosende s/n, 36280-Vigo, Spain (nati@dma.uvigo.es, durany@dma.uvigo.es).

‡Departamento de Matemática Aplicada, Facultad de Matemáticas, Universidad Complutense de Madrid, 28004-Madrid, Spain (ji_diaz@mat.ucm.es).

§Departamento de Ciencias Experimentales e Ingeniería, E.S.C.E.T. Universidad Rey Juan Carlos, E 28933, Móstoles, Madrid, Spain (eschiavi@escet.urjc.es).

¶Departamento de Matemáticas, Facultad de Informática, Universidade da Coruña, Campus Elviña s/n, 15071-A Coruña, Spain (carlosv@udc.es).

boundary defined by the model. The quantitative analysis is done in section 5, where we numerically solve the problem by using, among other techniques, the algorithm proposed in Bermúdez and Moreno [8]. Some numerical tests are then performed, and additional information is provided by the consideration of specific real data. Finally, in section 6, we discuss our results and their scope.

2. Model equation and strong formulation. The model equation is the one proposed in Fowler [29], describing the evolution of the thickness $h(t,x)$ for a two-dimensional plane ice sheet. ($z = h(t,x)$ is the top surface of the ice sheet.) Ice is taken to be incompressible, and the flow is very slow. It flows as a viscous medium under its own weight, owing to gravity. A number of additional simplifying assumptions are used in the derivation of the model we consider (isothermal flow, shallow ice approximation, a flat, rigid, and impermeable bed, etc.). We refer to [29] for details on the modelling; for a more general introduction to glaciology, see, for instance, Hutter [32], Paterson [36], and Lliboutry [33]. According Fowler [29], the local thickness of the ice sheet satisfies the following nonlinear diffusion equation:

$$h_t = \left(\frac{h^{n+2}}{n+2} |h_x|^{n-1} h_x - u_b h \right)_x + a \quad \text{on } I(t), \tag{2.1}$$

where $a = a(t,x)$ is a given scaled fixed accumulation-ablation rate function ($a < 0$ signifies ablation) and u_b is a (given) function representing the basal velocity. For each fixed t the domain $I(t)$ represents the (unknown) bounded real interval where $h(t,x) > 0$ (i.e., $I(t) := \{x \,/\, h(x,t) > 0\}$). Notice that the physically relevant rate functions $a(t,x)$ are changing sign functions, which are positive in the central (accumulation) region of the ice sheet and negative near the margins (the boundaries of $I(t)$, i.e., in the ablation region); see Fowler [30, p. 95]. The exponent n that appears in (2.1) represents the so-called Glen's exponent, and it is usually assumed that $n \approx 3$ (see Fowler [29]). We shall assume $n = 3$, but the qualitative analysis remains unchanged for any $n > 1$ (non-Newtonian case). As regards the appropriate (mechanical) boundary condition, it depends on the thermal regime which we consider at the base. There are two possible geophysical situations corresponding to slip or no slip conditions. We shall consider both of them, generalizing in this way Fowler's approach.

When basal ice reaches the melting point, there is a net heat flux arriving at the bed of the ice sheet, and consequently basal melt water is produced: the ice begins to slide. Sliding is expected only where the basal ice is at the melting point. When u_b (the sliding velocity) is a prescribed function of (t,x) (i.e., $u_b = u_b(t,x)$), this equation is a nonlinear diffusion-convection equation for h. It corresponds to slip conditions along an assumed temperate bed (warm-based ice sheet). Once the base reaches the melting point, we assume that the ice above remains cold. Our aim is to show how it is possible to solve this model for a general, prescribed velocity field. For a slow shallow flow over a flat cold base, there is no sliding (i.e., $u_b \equiv 0$), and the isothermal ice sheet equation (2.1) becomes just

$$h_t = \left(\frac{h^{n+2}}{n+2} |h_x|^{n-1} h_x \right)_x + a \quad \text{on } I(t). \tag{2.2}$$

We shall refer to (2.2) as the pure diffusive case. As discussed in Fowler [29], when a cold-based flow regime is considered and the no slip condition is prescribed (due to infinite slope), singularities appear at the margins during the advance of fronts of

a land-based ice sheet (such as the one which covered North America in the last ice age). Classical (finite-differences) numerical methods can fail. A further complication arises due to the fact that the domain where the equation holds is unknown. In fact it has to be determined as part of the solution.

The original *strong* formulation can be stated in the following terms: let $T > 0$, $L > 0$ be positive fixed real numbers, and let $\Omega = (-L, L)$ be an open bounded interval of $\mathbb{R}$ (a sufficiently large, fixed spatial domain). Given an accumulation-ablation rate function $a = a(t,x)$, an eventually zero sliding velocity function $u_b = u(t,x)$ defined on a large fixed parabolic domain $Q = (0,T) \times (-L,L)$, and an initial thickness $h_0 = h_0(x) \geq 0$ (bounded and compactly supported) on Ω, find two curves $S_+, S_- \in C^0([0,T])$, with $S_-(t) \leq S_+(t)$, a set $I(t) := (S_-(t), S_+(t)) \subset \Omega$ for any $t \in [0,T]$, and a sufficiently smooth function $h(t,x)$ defined on the set $Q_T := \bigcup_{t\in(0,T)} I(t)$ such that

$$(2.3) \qquad (\mathrm{SF}) := \begin{cases} h_t = \left[\dfrac{h^{n+2}}{n+2}|h_x|^{n-1}h_x - u_b h\right]_x + a & \text{in } Q_T, \\ h = 0 \quad \text{on } \{S_-(t)\} \cup \{S_+(t)\}, & t \in (0,T), \\ h = h_0 & \text{on } I(0), \end{cases}$$

and $h(t,x) > 0$ on Q_T. Notice that, for each fixed $t \in (0,T)$, $I(t) = (S_-(t), S_+(t)) = \{x \in \Omega : h(t,x) > 0\}$ denotes the ice-covered region. The curves $S_\pm(t)$ are called the interface curves or free boundaries associated with the problem and are defined by

$$S_-(t) = \mathrm{Inf}\{x \in \Omega : h(t,x) > 0\}, \qquad S_+(t) = \mathrm{Sup}\{x \in \Omega : h(t,x) > 0\}.$$

These curves define the interface separating the regions in which $h(t,x) > 0$ (i.e, ice regions) from those in which $h(t,x) = 0$ (i.e., ice-free regions). In the physical context they represent the propagation fronts of the ice sheet. The above formulation needs two different refinements. First, we have to prescribe some additional information on the spatial derivative of h at the free boundary. (We shall assume that the ice flux is zero there; see (3.2).) To introduce the other refinement it is useful to recall that many other examples of degenerate equations are typical of slow phenomena and satisfy the finite speed of propagation property (see, e.g., Díaz [17]).

Assuming $a \equiv 0$, for instance, if h_0 has a compact support, then $h(t,.)$ also has a compact support in $\mathbb{R}$ for any $t \in [0,T]$. So, if $a \equiv 0$, the domain Q_T can be found through the support of the solution $h(t,x)$ of the doubly nonlinear parabolic equation over the whole space $(0,T) \times \mathbb{R}$ and satisfying the initial condition $h(0,x) = h_0(x)$, $x \in \mathbb{R}$. Unfortunately, the physically relevant case, $a \not\equiv 0$, is much more complicated. Indeed, the finite speed of propagation still holds if $a(t,.)$ has compact support in $\mathbb{R}$ (for fixed $t \in (0,T)$). Moreover, in that case it can be shown that $\mathrm{supp}(h(t,.)) \subset \mathrm{supp}(a(t,.))$, and therefore $a(t,.)$ vanishes on the free boundary. Nevertheless, in glaciology models it is well known (see Fowler [30, p. 95]) that $a(t,.) < 0$ near the free boundaries (i.e., the margins of the ice sheet), and so there must exist another reason (other than the degenerate character of the equation) justifying the occurrence of the free boundaries $S_-(t), S_+(t)$. This is a mathematical modelling problem. We must make sure that the mathematical solutions are nonnegative compactly supported solutions (i.e., physically admissible). In short, for a sufficiently large fixed spatial domain, the physically admissible solutions are compactly supported nonnegative bounded functions such that $a < 0$, where $h = 0$ (in

particular, in the free boundary), and this is not predicted by the solutions of the diffusion equation (despite its degenerate character). Mathematically it is then possible (for special choices of the accumulation/ablation rate function) to have negative (no physically admissible) solutions corresponding to negative thickness! A practical way to overcome these inconsistencies is proposed in the following section.

3. Weak formulations. In this section we show that proper mathematical modelling in terms of weak formulations of the physical problem must be considered if the assumed physics have to be respected (i.e., if just physically admissible solutions have to be computed).

Let T, L, and Ω be as before and set $Q := (0,T) \times \Omega \subset \mathbb{R}^2$. The new model we present is based upon the fact that we can extend the function $h(t,x)$ outside of Q_T (the ice-covered regions) by zero on $Q \setminus Q_T = [(0,T) \times \Omega] \setminus Q_T$ (the complementary ice-free region). This extension still satisfies a nonlinear equation (this time of multivalued type) having the great advantage of being defined on an a priori known domain $Q = (0,T) \times \Omega$ (whose parabolic boundary is $\Sigma = \partial Q = (0,T) \times \partial\Omega$). This type of problem is known in the literature as an *obstacle problem*. In our case the obstacle function is $\psi \equiv 0$, the null function. Obstacle problems arise in many contexts related to friction, elasticity, thermodynamics, and so on (see, e.g., Duvaut and Lions [27] for further details). The multivalued formulation we propose appeared first in Díaz and Schiavi [21] (where the no slip condition was considered) to describe the slow, isothermal, one-dimensional flow of *cold* ice (i.e., all the ice is below melting point and the melting point is reached only at the bed) along a *hard* (i.e., rigid, impermeable) bed. Our results can be generalized to deal with the two-dimensional case that describes the evolution of a three-dimensional ice sheet. Here we extend that model to consider (prescribed) sliding along a temperate base. This introduces a nonlinear convective term into the multivalued equation which describes the movement of the ice masses. In order to properly characterize the behavior of h near the free boundary, we assume that the ice flux is not singular in the sense that

$$\frac{h^{n+2}}{n+2}|h_x|^{n-1}h_x - u_b h \in L^1(Q). \tag{3.1}$$

Notice that, formally, this implies

$$(h^m)_x = 0 \quad \text{on} \quad \{S_-(t)\} \cup \{S_+(t)\}, \quad t \in (0,T), \tag{3.2}$$

where $m = 2(n+1)/n$. Introducing the maximal monotone graph of $\mathbb{R}^2$, β, defined by

$$\beta(r) = \emptyset \text{ (the empty set) if } r < 0, \quad \beta(0) = (-\infty, 0], \quad \beta(r) = 0 \text{ if } r > 0, \tag{3.3}$$

the *obstacle formulation* (written in terms of a multivalued equation) is the following: given a bounded, sufficiently large interval $\Omega = (-L, L) \subset \mathbb{R}$, a rate function $a \in L^\infty(Q)$, a sliding velocity $u_b \in L^\infty(Q)$, and a compactly supported initial data $h_0 \in L^\infty(\Omega)$, find a sufficiently smooth function $h(t,x)$ which is a solution of

$$(\mathrm{MF}) := \begin{cases} h_t - \left(\dfrac{h^{n+2}}{n+2}|h_x|^{n-1}h_x - u_b h\right)_x + \beta(h) \ni a(t,x) & \text{in } Q, \\ h(t,x) = 0 & \text{on } \Sigma, \\ h(0,x) = h_0(x) & \text{on } \Omega. \end{cases} \tag{3.4}$$

Notice that β is multivalued just where h is zero, i.e., at the free boundaries. Moreover, by definition (3.3), we have that $0 \in \beta(0)$. Now, let h be a solution (in a weak sense to be specified later) of (3.4), for almost every $x \in \Omega$ and $\forall t \in (0,T)$. It is clear that in the null set $Q \setminus Q_T$ we must have $\beta(0) \ni a(t,x)$. This condition shows that, if β is multivalued at the origin, then it is possible to have solutions with a nonempty null set (i.e., $Q \setminus Q_T \neq \emptyset$) corresponding to equations in which $a \neq 0$ on $Q \setminus Q_T$, and thus new results are possible with respect to the single valued case ($\beta \equiv 0$).

Details on this kind of (multivalued) formulations, (MF), and maximal monotone graphs can be found in Brezis [11]. It is well known that the multivalued equation (3.4) can be written in terms of the so-called *complementarity formulation* for obstacle problems, which states: given Ω, a, u_b, and h_0 as before, find a sufficiently smooth function h such that

$$
(3.5)\qquad (\mathrm{CF}) := \begin{cases} h_t - \left(\dfrac{h^{n+2}}{n+2}|h_x|^{n-1}h_x - u_b h\right)_x - a \geq 0 & \text{in } Q, \\ \left[h_t - \left(\dfrac{h^{n+2}}{n+2}|h_x|^{n-1}h_x - u_b h\right)_x - a\right] h = 0 & \text{in } Q, \\ h \geq 0 & \text{in } Q, \\ h = 0 & \text{on } \Sigma, \\ h = h_0(x) & \text{on } \Omega. \end{cases}
$$

It is obvious that if a regular function h verifies the strong formulation, then its extension by zero over $Q \setminus Q_T$ (which we will denote again by h) satisfies trivially the complementarity formulation, assuming that $a(t,x)$ satisfies the condition

$$
a(t,x) \leq 0 \qquad \text{on} \quad Q \setminus Q_T.
$$

A more general framework is obtained if we define $\phi(r) = |r|^{n-1}r$, $r \in \mathbb{R}$, $n > 1$, and $\psi(s) = s^m$, with $s \geq 0$ and $m = 2(n+1)/n > 1$. (In fact, the existence and the uniqueness of solutions and some qualitative properties remain true if we replace ϕ by any real continuous strictly increasing convex function such that $\phi(0) = 0$, and β as before; see (3.3).) Introducing the new variable $u = u(t,x)$ and the real function $b(s)$ in form

$$
(3.6)\qquad u := h^m = \psi(h) \qquad \Longrightarrow \qquad u^{1/m} = h = \psi^{-1}(u) := b(u),
$$

we have $\phi(\psi(h)_x) = \phi(u_x) = |u_x|^{p-2}u_x$, where $p = n+1$. The previous *multivalued formulation* is the following: given Ω, a, u_b, and $u_0 = \psi(h_0)$ as before and a constant $\mu = n^n/[2^n(n+1)^n(n+2)]$, determine a function $u(t,x) = \psi(h(t,x))$ which is the solution of

$$
(3.7)\qquad (\mathrm{GF}) := \begin{cases} b(u)_t - [\mu\phi(u_x) - u_b b(u)]_x + \beta(u) \ni a(t,x) & \text{in } Q, \\ u(t,x) = 0 & \text{on } \Sigma, \\ b(u(0,x)) = b(u_0(x)) & \text{on } \Omega. \end{cases}
$$

This *general formulation*, (GF), is the one that we shall use to deal with the well-posedness of the model problem (3.4). Notice that we can write $\beta(u)$ instead of $\beta(b(u))$ because $\beta(u) \equiv \beta(h) := \beta(b(u))$ in Q. The equivalence is readily understood, observing that h (i.e., the original variable) and u have exactly the same support. The same remark applies to the boundary condition on Σ.

3.1. On the existence and uniqueness of weak solutions. Problem (3.7) admits various notions of solutions according to the required spatial and time regularity. In any case we must start by assuming some regularity on the data $a(t,x)$, $u_b(t,x)$, and $u_0(x)$. In our case it will be enough to assume that

$$a \in L^\infty(Q), \qquad u_b \in L^\infty(0,T : W^{1,\infty}(\Omega)), \qquad \text{and} \quad u_0 \in L^\infty(\Omega). \tag{3.8}$$

Motivated by (3.1), a natural notion of weak solution is the following.

DEFINITION 3.1. *A function $u \in L^1(Q)$ is a weak solution of* (3.7) *if $u \in L^p(0,T : W_0^{1,p}(\Omega))$, $b(u) \in L^1(Q)$, $u(t,x) \geq 0$ a.e. $(t,x) \in Q$, and there exists a function $j \in L^1(Q)$ such that $j(x,t) \in \beta(u(t,x))$ a.e. $(t,x) \in Q$ and*

$$\int_Q (\zeta_t b(u) - \zeta j + \zeta a) dxdt + \int_\Omega \zeta(0,\cdot) b(u_0) dx = \int_Q \zeta_x [\mu\phi(u_x) - u_b b(u)] dxdt$$

for any $\zeta \in L^p(0,T : W_0^{1,p}(\Omega)) \cap L^\infty(Q)$, $\zeta_t \in L^\infty(Q)$, and $\zeta(T,\cdot) = 0$.

Assuming (3.8) and that b, ϕ are the power functions indicated above, the existence of a weak solution can be obtained by different methods, for instance, by an easy modification of Theorem 2.3 and Proposition 3.2 of Benilan and Wittbold [4]. In fact, in order to check assumption (H1) of [4] it is useful to replace function b by its truncation

$$b_M(r) := \begin{cases} b(r) & \text{if } r \in [0,M], \\ b(M) & \text{if } r \in [M,+\infty), \end{cases}$$

with $M > 0$ an upper bound of any weak solution. (We shall come back to this point later; see Proposition 3.3.) Proving the uniqueness of (and the comparison principle for) weak solutions is a more delicate task due to the presence of the nonlinear term $b(u)$. This type of result is well known (see, for instance, Díaz and de Thelin [18]) in the case in which we additionally know that the weak solution is differentiable with respect to time in the sense that $b(u)_t \in L^1(Q)$. (We recall that from the definition of weak solutions we know merely that $b(u)_t \in L^{p'}(0,T : W^{-1,p'}(\Omega)) + L^1(Q)$ with $p' := p/(p-1)$.) In order to get such results, a weaker notion was introduced in previous works by different authors (see Boccardo et al. [10] for the case of $b(u) = u$, and Carrillo and Wittbold [15] for a general nondecreasing function $b(u)$): the notion of a *renormalized solution*, coming originally from a different context (Di Perna and Lions [24]). In fact both notions coincide in the class of bounded functions $u \in L^\infty(Q)$, which is our case, as we shall prove in this section.

For the sake of simplicity in the exposition we assume that

$$u_b(t,\cdot) \quad \text{is spatially constant.} \tag{3.9}$$

So, by some trivial modifications of the results of Carrillo and Wittbold [15] we arrive at the following result.

THEOREM 3.2. *Assume a_i, u_b, and $u_{0,i}$ satisfying* (3.8) *and* (3.9) *for $i = 1,2$. Let u_i be weak solutions of problem* (3.7) *associated with the data a_i and $u_{0,i}$, respectively. Then for any $t \in [0,T]$*

$$\int_\Omega [b(u_1(t,\cdot)) - b(u_2(t,\cdot))]_+ dx \leq \int_\Omega [b(u_{0,1}) - b(u_{0,2})]_+ dx + \int_0^t \int_\Omega [a_1(s,x) - a_2(s,x)]_+ dxds,$$

where $[f]_+ = \max(f,0)$. In particular, $b(u_{0,1}) \leq b(u_{0,2})$ and $a_1(t,x) \leq a_2(t,x)$, on their respective domains of definition, implies that $b(u_1(t,x)) \leq b(u_2(t,x))$ for any

$t \in [0,T]$ and a.e. $x \in \Omega$. Consequently, there is at most one weak solution of problem (3.7).

We point out that the above comparison remains true even if the functions u_i are not homogeneous at the boundary but satisfy $u_1(t,x) \le u_2(t,x)$ for any $t \in [0,T]$ and a.e. $x \in \partial\Omega$. This is again a trivial modification of the result by Carrillo and Wittbold [15], which will be used in the following section.

The boundedness of the associated weak solutions can be deduced from the above comparison principle as follows.

PROPOSITION 3.3. *Let u be any weak solution of problem* (3.7)*; then*

$$\|u\|_{L^\infty(Q)} \le M_0, \tag{3.10}$$

with

$$M_0 := b^{-1}\left(\max\{\|b(u_0)\|_{L^\infty(\Omega)}, 1\} \exp T\left\{\left[\frac{\|a\|_{L^\infty(Q)}}{\max\{\|b(u_0)\|_{L^\infty(\Omega)}, 1\}} + \|(u_b)_x\|_{L^\infty(\Omega)}\right]\right\}\right).$$

Proof. We take as a candidate *supersolution* a spatially constant function of the form $u_2(t,x) := b^{-1}(Ce^{\lambda t})$ for some $C > 0$ and $\lambda \in \mathbb{R}$ to be determined. Then $u_1(t,x) \le u_2(t,x)$ for any $t \in [0,T]$ and a.e. $x \in \partial\Omega$ and $b(u_{0,1}) \le b(u_{0,2})$ holds if

$$C = \max\{\|b(u_0)\|_{L^\infty(\Omega)}, 1\}.$$

Finally, by substituting u by u_2 in (3.7), it is easy to check that

$$a_2(t,x) := \lambda C e^{\lambda t} + (u_b)_x(x) C e^{\lambda t},$$

and so condition $a_1(t,x) \le a_2(t,x)$ is satisfied if, for instance,

$$\lambda = C^{-1}\|a\|_{L^\infty(Q)} + \|(u_b)_x\|_{L^\infty(\Omega)},$$

which implies the result. □

We point out that although the application of the present version of the comparison principle given in the above theorem requires condition (3.9), the a priori estimate (3.10) can be obtained without using a comparison principle (see, for instance formula (13) of Benilan and Wittbold [4]), and so the boundedness of u remains true also when $(u_b)_x \neq 0$, as we shall consider later.

4. On the free boundary. In this section we shall study both thermal regimes at the base. In the first case the bed is assumed to be cold (below melting point). No sliding is prescribed (i.e., $u_b \equiv 0$), and the pure diffusive case is analyzed. Next, we assume the ice sheet to be warm-based; the bed is then temperate, and sliding is prescribed (i.e., $u_b = u_b(t,x)$). Here we are not concerned with the switching mechanism between cold-temperate dynamics. (Results in that direction can be found in Fowler and Schiavi [31] and Díaz and Schiavi [22].) Our aim is to qualitatively describe the behavior of the free boundaries by means of a priori estimates on the support of the solution.

4.1. The no slip condition (pure diffusive case): Existence of the free boundary and the waiting time property. In this section we shall prove the existence of a nonempty null set

$$N(h(t,\cdot)) := \left\{(t,x) \in \{t\} \times \frac{\Omega}{h(t,x)} = 0\right\}$$

for the (unique) solution $h(t,x)$ of the problem

$$\text{(4.1)}\qquad \begin{cases} h_t - \mu\phi(\psi(h)_x)_x + \beta(h) \ni a(t,x) & \text{in } Q, \\ h(t,x) = 0 & \text{on } \Sigma, \\ h(0,x) = h_0(x) & \text{on } \Omega, \end{cases}$$

which can be deduced from the general formulation (GF) written in terms of the original variable h and of the functions ϕ and ψ introduced before. Assuming extra regularity of the solution (i.e, $h \in C(\bar{Q})$), we are able to analyze a great number of geophysical phenomena related to location and evolution of the free boundary and associated with the behavior of the function $a(t,x)$.

We shall now deal with the existence and location of the free boundary defined by problem (4.1). To show the existence of a free boundary as well as to locally estimate its location, we will use a technique based on the comparison result of section (3.1), which consists of the construction of appropriate local super-sub solutions having compact support. Thus, for all $\epsilon > 0$, we define the set

$$\text{(4.2)}\qquad N_\epsilon(a(t,\cdot)) := \left\{(t,x) \in \{t\} \times \frac{\Omega}{a(t,x)} \leq -\epsilon\right\}$$

and the set $S_\epsilon(a(t,.)) = Q \setminus N_\epsilon(a(t,\cdot)$. Then we have the following result.

THEOREM 4.1. *Let $h \in C(\bar{Q})$, $h \geq 0$, be a solution of* (4.1), *and let ϵ be a small real positive number such that the set $N_\epsilon(a(t,.))$ is not empty. Then there exist $R > 0$ and $T_0 \geq 0$ such that $\forall t \geq T_0$ we have*

$$N(h(t,\cdot)) \supset \{(t_0,x_0) \in N_\epsilon(a(t_0,.)) : d(x_0, S_\epsilon(a(t,.))) \geq R\}.$$

Proof. The proof is based on an original idea of Evans and Knerr [28], which applies when $n = 1$ and $a(t,x) \equiv 0$. See also Díaz and Hernández [20] for its adaptation to the case $n > 1$. In our multivalued case, with $n > 1$ but $a(t,x) \not\equiv 0$, we argue as follows. We consider the set $N_\epsilon(a(t,.))$ and define the function

$$\tilde{h}(t,x) = \psi^{-1}\left(\eta(|x - x_0|) + \psi(U(t))\right),$$

where

$$\text{(4.3)}\qquad \eta(r) = c\, r^{\frac{p}{p-1}}, \qquad c = \frac{p-1}{p}\left(\frac{\epsilon}{2}\right)^{\frac{1}{p-1}},$$

and $U(t)$ is the (unique) solution of the initial value problem

$$\text{(4.4)}\qquad \begin{cases} U' + \frac{1}{2}\beta(U) \ni -\frac{\epsilon}{2}, \\ U(0) = ||h_0||_{L^\infty(\Omega)}. \end{cases}$$

It is easy to state that $U(t) = [-\frac{\epsilon}{2}t + ||h_0||_{L^\infty}]^+$, whence

$$U(t) \equiv 0 \qquad \forall t \geq T_0 = \frac{2}{\epsilon}||h_0||_{L^\infty(\Omega)}.$$

On the other hand, as by construction $\phi(\psi(\tilde{h})_x)_x = \phi(\eta_x)_x = \epsilon/2$, we have (in $N_\epsilon(a(t,.))$)

$$\tilde{h}_t - \mu\phi(\psi(\tilde{h})_x)_x + \beta(\tilde{h})$$

$$\equiv \frac{d}{dt}\left[\psi^{-1}\left(\eta(|x-x_0|)+\psi(U(t))\right)\right]-\mu\phi(\eta_x(|x-x_0|))_x+\beta\left(\psi^{-1}\left(\eta(|x-x_0|)+\psi(U(t))\right)\right)$$

$$\supseteq \frac{\psi'(U)}{\psi'\left(\psi^{-1}\left(\eta(|x-x_0|)+\psi(U(t))\right)\right)}U'-\mu\phi(\eta_x(|x-x_0|))_x+\frac{1}{2}\beta(\psi^{-1}(\eta(|x-x_0|)))+\frac{1}{2}\beta(U)$$

$$\supseteq U'+\frac{1}{2}\beta(U)-\mu\phi(\eta_x(|x-x_0|))_x+\frac{1}{2}\beta\left(\psi^{-1}(\eta(|x-x_0|))\right)\ni -\epsilon\geq a(t,x).$$

Using the comparison principle written in terms of the original variable h, the following estimate holds (see Benilan and Wittbold [4]):

$$||h||_{L^\infty(Q)}\leq ||h_0||_{L^\infty(\Omega)}+\int_0^t ||a||_{L^\infty(\Omega)}=M(t).$$

Then

$$||h||_{L^\infty(Q)}\leq M(t)\leq \tilde{h}(t,\cdot)\qquad \text{on } N_\epsilon(a(t,\cdot))$$

iff $\psi^{-1}\left(\eta((|x-x_0|))+\psi(U(t))\right)\geq M(t)$; i.e., $\eta(|x-x_0|)+\psi(U(t))\geq\psi(M(t))$. In particular, this is true if $c\,|x-x_0|^{\frac{p}{p-1}}\geq\psi(M(t))$; by (4.3) the above reads

$$|x-x_0|\geq \frac{\psi(M(T))^{\frac{p-1}{p}}}{\left(\frac{p-1}{p}\right)^{\frac{p-1}{p}}\left(\frac{\epsilon}{2}\right)^{\frac{1}{p}}}=R, \tag{4.5}$$

and (4.5) implies that $\tilde{h}\geq h$ on $\partial N_\epsilon(a(t,.))$. At $t=0$ we use the monotonicity of ψ^{-1}:

$$\tilde{h}(0,x)=\psi^{-1}\left(\eta(|x-x_0|)+\psi(U(0))\right)=\psi^{-1}\left(\eta(|x-x_0|)+\psi(||h_0||_{L^\infty})\right)$$

$$\geq\psi^{-1}\left(\psi(||h_0||_{L^\infty})\right)=||h_0||_{L^\infty}\geq h_0(x)\geq 0.$$

Summarizing, if $(t,x)\in N_\epsilon(a(t,\cdot))$ is such that $|x-x_0|\geq R$, then

$$h_t-\mu\phi(\psi(h)_x)_x+\beta(h)\ni a\leq\inf\left(\tilde{h}_t-\mu\phi(\psi(\tilde{h})_x)_x+\beta(\tilde{h})\right)\qquad \text{in}\quad N_\epsilon(a(t,\cdot)),$$

$$h(t,x)\leq\tilde{h}(t,x)\qquad \text{on}\quad \partial N_\epsilon(a(t,\cdot)),$$

$$h_0(x)\leq\tilde{h}(0,x)\qquad \text{on}\quad N_\epsilon(a(0,\cdot)).$$

Next, from the comparison result (Theorem 3.2) it follows that

$$0\leq h(t,x)\leq\tilde{h}(t,x)\qquad \text{in}\quad N_\epsilon(a(t,.)),$$

and we end up observing that $h(t,x_0)=0\ \forall t\geq T_0=\frac{2}{\epsilon}||h_0||_{L^\infty}$ and x_0 satisfies inequality (4.5), i.e., $(t,x_0)\in\{N_\epsilon(a(t,.))/|x-x_0|\geq R\}$. □

We shall now analyze the so-called waiting time property. As discussed in Fowler [30, p. 95], the slope of the surface is singular in advance but finite in retreat. This distinction causes the degenerate diffusion equation above to have waiting-time behavior, because following a retreat, the margin slope must rebuild itself before another advance it possible. The following property applies if the initial data is sufficiently *flat* in the *ablation region.*

THEOREM 4.2. *Let $h \in C(\bar{Q})$, $h \geq 0$, be a solution of problem (4.1). Let $\delta = \eta^{-1}(\psi(M))$ and $B_\delta^+(x_0) = \{x \in \Omega / \ x \in [x_0, x_0 + \delta)\}$, with $M = \|h\|_{L^\infty(Q)}$, $x_0 = S_+(0)$, $\tilde{c} = (\frac{p-1}{p})\epsilon^{\frac{1}{p-1}}$, and $\eta(|x - x_0|) = \tilde{c}\,|x - x_0|^{\frac{p}{p-1}}$. Assume that there exists $T^* > 0$ such that $a(t,x) \leq -\epsilon$ a.e. $x \in B_\delta^+(x_0)$ and $t \in (0, T^*)$. If $x_0 \in \Omega$ satisfies $0 \leq h_0(x_0) \leq \psi^{-1}(\eta(|x - x_0|))$, then*

$$\exists\, t^*, \quad 0 < t^* \leq T^*, \quad \textit{such that} \quad S_+(0) = S_+(t) \quad \forall t \in (0, t^*).$$

Proof. We define the function

$$\tilde{h}(x) := \psi^{-1}(\eta(|x - x_0|)) \qquad \text{in} \quad B_\delta^+(x_0) \times (0, T^*).$$

Then

$$h_t - \mu\phi(\psi(h)_x)_x + \beta(h) \ni a \leq -\epsilon \leq \inf\big(\tilde{h}_t - \mu\phi(\psi(\tilde{h})_x)_x + \beta(\tilde{h})\big) \quad \text{in } B_\delta^+(x_0) \times (0, T^*).$$

On $\partial B_\delta^+(x_0) \times [0, t^*]$ we have to verify that $h \leq M \leq \tilde{h} = \psi^{-1}(\eta)$, and this is iff $\psi(M) \leq \eta = \tilde{c}|x - x_0|^{\frac{p}{p-1}}$. On ∂B_δ^+ this reads as $\psi(M) \leq \tilde{c}\delta^{\frac{p}{p-1}}$. Using that $\delta = \eta^{-1}(\psi(M))$,

$$h \leq M \leq \tilde{h} \iff \psi(M) \leq \tilde{c}[\eta^{-1}(\psi(M))]^{\frac{p}{p-1}}$$

$$\iff \left[\frac{\psi(M)}{\tilde{c}}\right]^{\frac{p-1}{p}} \leq \eta^{-1}(\psi(M)) \iff \eta\left(\left[\frac{\psi(M)}{\tilde{c}}\right]^{\frac{p-1}{p}}\right) \leq \psi(M),$$

and this is always verified as can be deduced by applying the definition of the function η. Then we have

$$h_t - \mu\phi(\psi(h)_x)_x + \beta(h) \ni a \leq \inf(\tilde{h}_t - \mu\phi(\psi(\tilde{h})_x)_x + \beta(\tilde{h})) \text{ in } B_\delta^+(x_0) \times (0, t^*),$$

$$h(x_0, 0) = h_0(x_0) \leq \tilde{h}(x) = \psi^{-1}(\eta(|x - x_0|)) \quad \text{on } B_\delta^+(x_0),$$

$$h(t,x) \leq M \leq \tilde{h}(x) \quad \text{on } \partial B_\delta^+(x_0) \times (0, t^*).$$

Finally, the comparison result shows that $0 \leq h(t,x) \leq \tilde{h}(x)$, and so $h(t, x_0) \equiv 0$ $\forall t \in (0, t^*)$. □

4.2. The slip condition (diffusive-convective case): Existence of the free boundary and the waiting time property. In this section we shall consider the general formulation (GF), assuming that $u_b \not\equiv 0$ and without assuming (3.9). Even if Theorem 3.2 can be extended to cover cases in which (3.9) is not satisfied, the presence of the convection term makes the method of super- and subsolutions very hard to apply. Thus, in order to prove the existence of the free boundary, we shall use a different technique called the *energy method*. It has been developed by different authors in the last twenty years for the study of nonlinear problems for which the maximum principle fails (see, for instance, the monograph of Antontsev, Díaz, and Shmarev [2]). In fact, although this energy method can be applied in different ways, we shall follows the ideas introduced in Díaz and Galiano [19] in order to apply the method to some fluid dynamics problems. We start by pointing out that the equation of problem (3.7) can be written in terms of a nonconservative transport multivalued equation in the form

$$b(u)_t + u_b b(u)_x - \mu\phi(u_x)_x + (u_b)_x b(u) + \beta(u) \ni a(t,x) \qquad \text{in} \quad Q. \tag{4.6}$$

In this way, the equation involves the material derivative $b(u)_t + u_b b(u)_x$, which can be associate to a *virtual non-Newtonian fluid with a reactive term* $(u_b)_x b(u) + \beta(u)$. We shall prove the existence of the free boundary in terms of the so-called *finite speed of propagation* near a given point x_0.

In the next results we shall assume that u_b is a globally Lipschitz continuous function. Thus, we can define the characteristics of the associate flow by

$$\text{(4.7)} \qquad \begin{cases} \dfrac{d}{dt}X(t,x) &= u_b(t, X(t,x)) \qquad \text{on} \quad (0,T), \\ X(0,x) &= x. \end{cases}$$

As usual in continuum mechanics, given a ball $B_\rho(x_0) = \{x \in \mathbb{R} : |x - x_0| \le \rho\}$, we denote the transformed set by

$$B_\rho(x_0)_t = \{\, y \in \mathbb{R} : y = X(t,x) \quad \text{for some} \quad x \in B_\rho(x_0)\}.$$

THEOREM 4.3. *Let b, ϕ, β, a, and u_0 be as in section 3. Let u_b be a globally Lipschitz continuous function on Q. For $\epsilon \ge 0$ let $N_\epsilon(a(t,\cdot)) := \{(t,x) \in \{t\} \times \Omega / a(t,x) \le -\epsilon\}$. Assume also that $\epsilon = 0$ if $m(p-1) > 1$, and $\epsilon > 0$ if $m(p-1) \le 1$. Let $u_0 = 0$ on a ball $B_{\rho_0}(x_0)$ for some x_0 such that $(t, B_{\rho_T}(x_0)) \subset N_\epsilon(a(t,\cdot))$ for any $t \in [0,T]$ and some $L \ge \rho_0$. Then there exists a $T_\epsilon \in (0,T]$ and a function $\rho : [0,T_\epsilon] \to [0,\rho_0]$ such that $u(t,x) = 0$ a.e. $x \in B_{\rho(t)}(x_0)$ for any $t \in [0,T_\epsilon]$.*

Proof. We introduce the change of variable $b(w(t,x)) = b(u(t,x))e^{\lambda t}$. Then, it is easy to prove that w satisfies the equation

$$\text{(4.8)} \qquad \begin{aligned} &b(w)_t + u_b b(w)_x - \mu e^{\lambda t(1-(p-1)m)}\phi(w_x)_x + [(u_b)_x + \lambda]b(w) + \beta(w) \\ &\ni a(t,x)e^{\lambda t} \qquad \text{in} \quad Q. \end{aligned}$$

Thus, by taking $\lambda > 2C$ with $C = \|(u_b)_x\|_{L^\infty(Q)}$ (which is finite, since u_b is a globally Lipschitz continuous function), we have that $[(u_b)_x + \lambda] \ge C > 0$. By multiplying, formally, by w (i.e., by some arguments of regularization, localization, and passing to the limit, as in Díaz and Veron [23]), we get that if $\rho \le L$, then

$$\int_{B_\rho(x_0)_t} \frac{\partial}{\partial t}\Psi(w)dx + \int_{B_\rho(x_0)_t} u_b \Psi(w)_x dx + \mu e^{\lambda t(1-(p-1)m)} \int_{B_\rho(x_0)_t} |w_x|^p \, dx$$

$$\le \mu e^{\lambda t(1-(p-1)m)} w(t,\cdot)\,|w_x(t,\cdot)|^{p-1}\, w_x(t,\cdot)\,\big|_{\partial B_\rho(x_0)_t} - \epsilon \int_{B_\rho(x_0)_t} w dx,$$

where

$$\text{(4.9)} \qquad \Psi(w) := wb(w) - \int_0^w b(s)ds$$

and we used that $w \ge 0$ and that $\beta(w)w = \{0\}$. Now, by using the Reynolds transport lemma,

$$\int_{B_\rho(x_0)_t} \frac{\partial}{\partial t}\Psi(w) + \int_{B_\rho(x_0)_t} u_b \Psi(w)_x = \frac{d}{dt}\int_{B_\rho(x_0)_t} \Psi(w(t,y))dy.$$

Thus, integrating in $(0,t)$ and using the information on u_0, we get that

$$\int_{B_\rho(x_0)_t} \Psi(w(t,y))dy + C_1 \int_0^t \int_{B_\rho(x_0)_t} |w_x|^p \, dyds$$

$$\leq C_2 \int_0^t w(s,\cdot)\left||w_x(s,\cdot)|^{p-1}\, w_x(s,\cdot)\,|_{\partial B_\rho(x_0)_t}\right| ds - \epsilon \int_0^t \int_{B_\rho(x_0)_t} w dx ds, \tag{4.10}$$

with

$$C_1 = \mu \min_{t\in[0,T]} e^{\lambda t(1-(p-1)m)}, \qquad C_2 = \mu \max_{t\in[0,T]} e^{\lambda t(1-(p-1)m)}.$$

Assume now, for the moment, that $1 < (p-1)m$ and $\epsilon = 0$. Then we define the energies

$$B(t,\rho) = \sup_{0\leq s\leq t} \int_{B_\rho(x_0)s} \Psi(w(s,y))dy, \qquad E(t,\rho) = \int_0^t \int_{B_\rho(x_0)_t} |w_x|^p\, dyds. \tag{4.11}$$

Using Hölder inequality and the interpolation-trace inequality of Díaz and Veron [23], we get that

$$B + E \leq K\left(\frac{\partial E}{\partial \rho}\right)^{\omega} \tag{4.12}$$

for some positive constant K and some $\omega > 1$, and the result follows in a standard way (see, e.g., Díaz and Veron [23], or Antontsev, Díaz, and Shmarev [2]). In the case $1 \geq (p-1)m$ and $\epsilon > 0$ we pass the term $\epsilon \int_0^t \int_{B_\rho(x_0)_t} w dx ds$ to the left-hand side of the inequality (4.10), and we introduce the additional energy function defined as

$$C(t,\rho) = \int_0^t \int_{B_\rho(x_0)_t} |w|\, dyds.$$

(Remember that $|w| = w$.) Then, we can apply Theorem 1 of Antontsev, Díaz, and Shmarev [1], with $\lambda = 0$ since the interpolation-trace inequality (2.6) of that paper applies also to the limit case $\lambda = 0$. Thus, we arrive at the inequality

$$E + C \leq K\left(\frac{\partial (E+C)}{\partial \rho}\right)^{\omega} \tag{4.13}$$

for some positive constant K and some $\omega > 1$, and the theorem holds. □

Remark 4.1. We point out that, due to the presence of the convective term and the specific exponents involved in (4.6), the statement of the parabolic part of Díaz and Veron [23] is not directly applicable, and this is the reason for using the characteristic transformation argument. Notice, also, that in contrast with the case $u_b = 0$, now it may occur that $T_\epsilon < T$ for any $\epsilon \geq 0$, and notice too that the energy method allows the consideration of the case $\epsilon = 0$ when $m(p-1) > 1$. Moreover, any estimate of the function $\rho(t)$ automatically gives an estimate on the location of the free boundary. Finally, we indicate that it is possible to get global consequences of the above result by estimating (globally) the energies introduced in (4.11). (For some related arguments, see, e.g., Díaz and Veron [23] or Antontsev, Díaz, and Shmarev [2].) Unfortunately the above information on the free boundary is quite implicit and difficult to manage. This also justifies the use of numerical methods.

The waiting time property can also be studied by energy methods once it is reformulated in terms of the characteristics associated with u_b. Notice that if $u_b \equiv 0$, then the characteristics are vertical lines.

THEOREM 4.4. *Let b, ϕ, β, a, u_b, ϵ, $N_\epsilon(a(t,\cdot))$, and x_0 be as in the previous theorem but now with $L > \rho_0$. Let $u_0(x) = 0$ on a ball $B_{\rho_0}(x_0)$ for some x_0 and satisfying that*

$$\int_{B_\rho(x_0)_t} \Psi(u_0(y))dy \le \theta[(\rho-\rho_0)^+]^{\omega/(\omega-1)} \qquad \text{for any} \quad \rho_0 \le \rho \le L \tag{4.14}$$

for some small enough $\theta > 0$ and some $L > \rho_0$, where Ψ is defined by (4.9) and $\omega > 1$ is the exponent given in (4.12) or (4.13). Then, there exists $T_0 \in (0,T]$ such that $u(t,x) = 0$ a.e. $x \in B_{\rho_0}(x_0)_t$ for any $t \in [0,T_0]$, where $B_{\rho_0}(x_0)_t = \{y \in \mathbb{R} : y = X(t,x)$ for some $x \in B_{\rho_0}(x_0)\}$, with $X(t,x)$ the characteristics defined by (4.7).

Proof. The proof follows from the same arguments as those used by Antontsev, Díaz, and Shmarev [1], but adapted to our framework. Thus, the integration by parts formula (4.10) must be replaced by

$$\begin{aligned} &\int_{B_\rho(x_0)_t} \Psi\,(w(t,y))dy + C_1 \int_0^t \int_{B_\rho(x_0)_t} |w_x|^p\, dyds \\ &\qquad \le \int_0^t w(s,\cdot) \left| |w_x(s,\cdot)|^{p-1} w_x(s,\cdot) \right|_{\partial B_\rho(x_0)_t} \Big| ds \\ &\qquad\quad - \epsilon \int_{B_\rho(x_0)_t} w dx + \int_{B_\rho(x_0)_t} \Psi(u_0(y))dy. \end{aligned} \tag{4.15}$$

In particular, inequality (4.12) becomes the nonhomogeneous one,

$$B + E \le K \left(\frac{\partial E}{\partial \rho} \right)^{\omega} + \theta(\rho - \rho_0)_+^{\omega/(\omega-1)},$$

and the conclusion holds thanks to a technical lemma (see, e.g., Lemma 1 of Antontsev, Díaz, and Shmarev [1]). □

5. Numerical solution. This section is devoted to the numerical solution of the ice sheet moving boundary problem whose multivalued formulation (MF) is stated in (3.4). We first introduce the total derivative notation in conservative form,

$$\frac{Dh}{Dt} = \frac{\partial h}{\partial t} + \frac{\partial}{\partial x}(u_b h),$$

so that the complementarity formulation (CF) given by (3.5) can be posed as

$$\begin{cases} \dfrac{Dh}{Dt} - \left(\dfrac{h^{n+2}}{n+2} |h_x|^{n-1} h_x \right)_x - a \ge 0 & \text{in} \quad Q, \\ \left[\dfrac{Dh}{Dt} - \left(\dfrac{h^{n+2}}{n+2} |h_x|^{n-1} h_x \right)_x - a \right] h = 0 & \text{in} \quad Q, \\ h \ge 0 & \text{in} \quad Q, \\ h = 0 & \text{on} \quad \Sigma, \\ h = h_0(x) & \text{on} \quad \Omega. \end{cases} \tag{5.1}$$

An overview of different numerical strategies for solving free boundary problems (fixed domain methods, front-tracking, and front-fixing methods, adaptative algorithms, and others) can be found in [34]. Our approach is based on fixed domain

methods, upwinding time discretization, and duality methods for nonlinearities. More precisely, in the recent paper [13] a first attempt was made to solve (5.1) by combining this approach with a fixed point method for the nonlinear diffusive term. Indeed, the linearization process was based on freezing the nonlinear diffusive term at each step of the algorithm.

In the subsequent paper [14], in order to solve a temperature-profile coupled problem, this method was combined with the algorithm proposed in [12] to approximate ice sheet temperature distribution. However, this profile approximation procedure requires extremely small time steps and, consequently, it leads to very high computing times to obtain an accurate stationary solution.

In the present work, to overcome the drawbacks of the previously described numerical approach, we express the nonlinear diffusive term by means of a monotone operator. As usual in glaciology (see section 2), let $n = 3$. Hence, $m = 2(n+1)/n = 8/3 > 1$ and $p = n + 1 = 4$. Then, by using (3.6), we introduce the following new variable u,

$$u(t,x) = h^{8/3}(t,x), \tag{5.2}$$

so that problem (5.1) can be written in terms of u as

$$\begin{cases} \dfrac{D}{Dt}(u^{3/8}) - \mu \left(|u_x|^2 u_x\right)_x - a \geq 0 & \text{in } Q, \\ \left[\dfrac{D}{Dt}(u^{3/8}) - \mu \left(|u_x|^2 u_x\right)_x - a\right] u = 0 & \text{in } Q, \\ u \geq 0 & \text{in } Q, \\ u = 0 & \text{on } \Sigma, \\ u = u_0(x) = h_0^{8/3}(x) & \text{on } \Omega, \end{cases} \tag{5.3}$$

where the constant μ takes the value $\mu = \frac{(3/8)^3}{5}$. Notice that formulation (5.3) allows us to introduce a maximal monotone operator to express the nonlinear diffusive term and implicitly contains a convective term.

In view of the particular nonlinear diffusive term in (5.3), the classical method analyzed in the framework of linear diffusion problems ($p = 2$) by Nochetto and Verdi [35] cannot be applied. In the same manner, the nonlinear diffusive terms treated in the recent paper [16] do not cover the case of (5.3).

In fact, the nonlinear p-Laplacian term has been numerically studied in [6] and the references therein, but without including either convection or free boundary aspects.

The combination of characteristic methods with duality algorithms for solving (5.3) is justified by its previous validation in analogous free boundary problems in other topics (lubrication [3, 25, 26], phase change [9], and gas flow [7], for example).

One goal of this work is to propose a numerical solution method for approximating the ice sheet profile for prescribed accumulation-ablation rates and the sliding velocity of ice. A further goal is to illustrate the qualitative properties that were analyzed in section 4.

5.1. Time semidiscretization. As in previous works in the glaciology setting [13, 14], problem (5.3) is discretized in time using the scheme of characteristics. For this, let T and M be fixed positive real numbers, and let Δt be the time step so that $T = M\Delta t$. In short, this upwinded time scheme is based on the approximation

of the total derivative; see Pironneau [37] for linear convection-diffusion equations. Thus, in our particular nonlinear convection case, for $m = 0, 1, \ldots, M (M = T/\Delta t)$, we consider the approximation

$$\frac{D}{Dt}(u^{3/8})((m+1)\Delta t, x) \approx \frac{(u^{m+1})^{3/8}(x) - J^m(x)\,(u^m)^{3/8}(\chi^m(x))}{\Delta t}, \tag{5.4}$$

where

$$u^{m+1}(x) = u((m+1)\Delta t, x) \quad \text{in} \quad \Omega \tag{5.5}$$

and $J^m(x)$ is obtained by numerical quadrature techniques in the expression

$$J^m(x) = J(t^{m+1}, x; t^m) = 1 - \int_{t^m}^{t^{m+1}} (u_b(\tau, \chi(x, t^{m+1}; \tau)))_x \, d\tau,$$

where J is the Jacobian associated with the change of variable mapping $x \to \chi(t, x; \tau)$. Notice that the presence of J arises from the application of the characteristics method when the convection is written in conservative form (see Bercovier, Pironneau, and Sastri [5] for details).

The value $\chi^m(x)$ is given by $\chi^m(x) = \chi((m+1)\Delta t, x; m\Delta t)$, χ being the solution of the final value problem

$$\begin{cases} \dfrac{d\chi(t, x; s)}{ds} &= u_b(s, \chi(x, t; s)), \\ \chi(t, x; t) &= x. \end{cases} \tag{5.6}$$

The next step consists of the substitution of the approximation (5.4) into (5.3) to obtain the following sequence of nonlinear elliptic complementarity problems.

For $m = 0, 1, 2, \ldots, M$, find u^{m+1} such that

$$\begin{cases} \dfrac{(u^{m+1})^{3/8} - J^m((u^m)^{3/8} \circ \chi^m)}{\Delta t} - \mu \dfrac{\partial}{\partial x}\left(|u_x^{m+1}|^2 u_x^{m+1}\right) - a^{m+1} \geq 0 \quad \text{in } \Omega, \\ u^{m+1} \geq 0 \quad \text{in } \Omega, \\ \left[\dfrac{(u^{m+1})^{3/8} - J^m((u^m)^{3/8} \circ \chi^m)}{\Delta t} - \mu \dfrac{\partial}{\partial x}\left(|u_x^{m+1}|^2 u_x^{m+1}\right) - a^{m+1}\right] u^{m+1} = 0 \quad \text{in } \Omega, \\ u^{m+1} = 0 \quad \text{in } \partial\Omega, \\ u^0(x) = h_0 = (h_0)^{8/3} \quad \text{in } \Omega, \end{cases} \tag{5.7}$$

where $a^{m+1}(x) = a((m+1)\Delta t, x)$ and "$\circ$" denotes the composition symbol.

5.2. Spatial discretization. First, in order to solve the nonlinear complementarity problem (5.7) to obtain u^{m+1}, we pose the following equivalent variational inequality formulation.

Find $u^{m+1} \in K$ such that

$$\begin{aligned} &\frac{1}{\Delta t}\int_\Omega (u^{m+1,})^{3/8}\,(\varphi - u^{m+1})\,dx + \mu \int_\Omega |\, u_x^{m+1}\,|^2\, u_x^{m+1}(\varphi - u^{m+1})_x dx \\ &\geq \frac{1}{\Delta t}\int_\Omega J^m\,((u^m)^{3/8} \circ \chi^m)(\varphi - u^{m+1})\,dx + \int_\Omega a^{m+1}\,(\varphi - u^{m+1})dx \\ &\forall \varphi \in K, \end{aligned} \tag{5.8}$$

where $K = \{\varphi \in W_0^{1,4}(\Omega) \,/\, \varphi \geq 0 \text{ a.e. in } \Omega\}$.

Next, the duality algorithm proposed in Bermúdez and Moreno [8] is applied to the variational inequality (5.8). For this, (5.8) is expressed in terms of the indicatrix function I_K of the convex K in the following form.

Find $u^{m+1} \in W_0^{1,4}(\Omega)$ *such that*

$$\frac{1}{\Delta t}\int_\Omega (u^{m+1})^{3/8}(\varphi - u^{m+1})dx + \mu\int_\Omega \mid u_x^{m+1} \mid^2 u_x^{m+1}(\varphi - u^{m+1})_x dx + I_K(\varphi) - I_K(u^{m+1})$$
$$\geq \frac{1}{\Delta t}\int_\Omega J^m\left((u^m)^{3/8} \circ \chi^m\right)(\varphi - u^{m+1})dx + \int_\Omega a^{m+1}(\varphi - u^{m+1})dx \qquad \forall \varphi \in W_0^{1,4}(\Omega). \tag{5.9}$$

Moreover, the use of subdifferential calculus leads to the equivalent formulation

$$\xi_1^{m+1} = -(\mathcal{A}(u^{m+1}) - f^m) \in \partial I_K(u^{m+1}), \tag{5.10}$$

where $\partial I_K(u)$ denotes the subdifferential of the convex function I_K at the point u; see Brezis [11] for more details. Moreover, the operator $\mathcal{A} : W_0^{1,4}(\Omega) \to W^{-1,4/3}(\Omega)$ is defined by

$$\langle \mathcal{A}(\varphi), \psi\rangle = \frac{1}{\Delta t}\int_\Omega \varphi^{3/8}\psi dx + \mu\int_\Omega \mid \varphi_x \mid^2 \varphi_x\psi_x dx,$$

and the element $f^m \in W^{-1,4/3}(\Omega)$ is defined by

$$\langle f^m, \psi\rangle = \int_\Omega a^{m+1}\psi dx + \frac{1}{\Delta t}\int_\Omega J^m((u^m)^{3/8} \circ \chi^m)\psi dx.$$

Therefore, (5.10) is equivalent to the following problem.

Find $u^{m+1} \in W_0^{1,4}(\Omega)$ *such that*

$$\frac{1}{\Delta t}\int_\Omega (u^{m+1})^{3/8}\,\psi\,dx + \int_\Omega \xi_1^{m+1}\,\psi\,dx + \mu\int_\Omega \xi_2^{m+1}\psi_x dx$$
$$-\frac{1}{\Delta t}\int_\Omega J^m((u^m)^{3/8} \circ \chi^m)\psi dx = \int_\Omega a^{m+1}\,\psi\,dx \qquad \forall \psi \in W_0^{1,4}(\Omega), \tag{5.11}$$

$$\xi_1^{m+1} \in \partial I_K\left[u^{m+1}\right], \tag{5.12}$$

$$\xi_2^{m+1} = \Lambda\left(\frac{\partial u^{m+1}}{\partial x}\right), \tag{5.13}$$

where $\Lambda(v) = \mid v \mid^2 v = v^3$.

The application of the Bermúdez–Moreno algorithm [8] to solving the nonlinear problem (5.11)–(5.13) introduces the following new unknowns (multipliers) q_1^{m+1} and q_2^{m+1},

$$q_1^{m+1} \in \partial I_K\left[u^{m+1}\right] - \omega_1 u^{m+1}, \tag{5.14}$$

$$q_2^{m+1} = \Lambda\left(\frac{\partial u^{m+1}}{\partial x}\right) - \omega_2\frac{\partial u^{m+1}}{\partial x}, \tag{5.15}$$

defined in terms of the positive parameters ω_1 and ω_2. So, (5.11) is equivalent to

$$\frac{1}{\Delta t}\int_\Omega (u^{m+1})^{3/8}\psi dx + \int_\Omega (q_1^{m+1}+\omega_1 u^{m+1})\psi\, dx + \mu\int_\Omega \left(q_2^{m+1}+\omega_2\frac{\partial u^{m+1}}{\partial x}\right)\frac{\partial \psi}{\partial x}\, dx$$
$$= \int_\Omega a^{m+1}\psi\, dx + \frac{1}{\Delta t}\int_\Omega J^m\left((u^m)^{3/8}\circ\chi^m\right)\psi dx \qquad \forall \psi \in W_0^{1,4}(\Omega). \tag{5.16}$$

Now, since ∂I_K and Λ are maximal monotone operators, the definitions given by (5.14) and (5.15) can be characterized by their respective identities (see [8]):

$$q_1^{m+1} = (\partial I_K)_{\lambda_1}^{\omega_1}\left[u^{m+1}+\lambda_1 q_1^{m+1}\right], \tag{5.17}$$

$$q_2^{m+1} = \Lambda_{\lambda_2}^{\omega_2}\left[\frac{\partial u^{m+1}}{\partial x}+\lambda_2 q_2^{m+1}\right]. \tag{5.18}$$

In (5.17) and (5.18), the functions $(\partial I_K)_{\lambda_1}^{\omega_1}$ and $\Lambda_{\lambda_2}^{\omega_2}$ denote the Yosida approximations for the operators $(\partial I_K - \omega_1 I)$ and $(\Lambda - \omega_2 I)$ with positive parameters λ_1 and λ_2, respectively (see Brezis [11], for example). Next, to discretize (5.16)–(5.18) in space, we consider piecewise linear Lagrange finite elements. More precisely, for a given positive parameter h we build a uniform finite element mesh τ_h for Ω. Thus, let $x_i = (i-1)h$, $i = 1,\ldots,N+1$, be the mesh nodes. Now, we introduce the classical finite elements spaces and sets:

$$\begin{aligned} V_h &= \{\varphi_h \in C^0(\Omega)\ /\ \varphi_h\,|_E \in P_1 \quad \forall E \in \tau_h\},\\ V_{0h} &= \{\varphi_h \in V_h\ /\ \varphi_h\,|_{\partial\Omega} = 0\},\\ K_h &= \{\varphi_h \in V_{0h}\ /\ \varphi_h(x_i) \geq 0, \quad i = 1,\ldots,N+1\}, \end{aligned} \tag{5.19}$$

where E denotes a standard finite element interval.

Then, the fully discretized problem can be posed as follows.

Find $u_h^{m+1} \in K_h$ such that

$$\begin{aligned} &\frac{1}{\Delta t}\int_\Omega (u_h^{m+1})^{3/8}\psi_h\, dx + \omega_1\int_\Omega u_h^{m+1}\psi_h\, dx + \mu\omega_2\int_\Omega \frac{\partial u_h^{m+1}}{\partial x}\frac{\partial \psi_h}{\partial x}\, dx\\ &= \int_\Omega a_h^{m+1}\,\psi_h\, dx + \frac{1}{\Delta t}\int_\Omega J^m((u_h^m)^{3/8}\circ\chi^m)\psi_h\, dx - \int_\Omega q_{1,h}^{m+1}\psi_h\, dx\\ &\quad - \mu\int_\Omega q_{2,h}^{m+1}\frac{\partial \psi_h}{\partial x}\, dx \quad \forall \psi_h \in V_{0h}. \end{aligned} \tag{5.20}$$

Thus, by treating the first term in (5.20) in explicit form at each step of the inner multipliers loop, the numerical algorithm for solving the fully discretized problem (5.20), (5.18), and (5.17) can be sketched as follows.

Step 0 : Initialize $(u_h^{m+1})_0$ (equal to u_h^m, for example)

Step j : For a given$(u_h^{m+1})_j$, compute $(u_h^{m+1})_{j+1} \in V_{0h}$ by solving the linear problem

$$\begin{aligned}
&\omega_1 \int_\Omega (u_h^{m+1})_{j+1}\psi_h \, dx + \mu\omega_2 \int_\Omega \frac{\partial (u_h^{m+1})_{j+1}}{\partial x}\frac{\partial \psi_h}{\partial x} \, dx \\
&= -\frac{1}{\Delta t}\int_\Omega (u_h^{m+1})_j^{3/8} \, \psi_h \, dx \; - \int_\Omega (q_{1,h}^{m+1})_j \, \psi_h \, dx - \mu \int_\Omega (q_{2,h}^{m+1})_j \frac{\partial \psi_h}{\partial x} dx \\
&+ \int_\Omega a_h^{m+1}\psi_h \, dx + \frac{1}{\Delta t}\int_\Omega J^m \left(((u_h^m)_j)^{3/8} \circ \chi^m\right) \psi_h \, dx \qquad \forall \psi \in V_{0h}.
\end{aligned} \tag{5.21}$$

The multipliers updating (indexed by j) is provided by the following expressions:

$$(q_{1,h}^{m+1})_{j+1} = (\partial I_K)_{\lambda_1}^{\omega_1}[(u_h^{m+1})_{j+1} + \lambda_1 (q_{1,h}^{m+1})_j], \tag{5.22}$$

$$(q_{2,h}^{m+1})_{j+1} = \Lambda_{\lambda_2}^{\omega_2}\left[\frac{\partial}{\partial x}(u_h^{m+1})_{j+1} + \lambda_2 (q_{2,h}^{m+1})_j\right]. \tag{5.23}$$

The convergence of the duality method is established in Bermúdez and Moreno [8] and Bermúdez [7] under the technical constraint $\lambda_i \omega_i = 0.5$ for $i = 1, 2$. For this particular choice of the parameters, the Yosida approximations can easily be computed and are given by

$$(\partial I_K)_{\frac{1}{2\omega_1}}^{\omega_1}(r) = -2\omega_1 \mid r \mid,$$

$$\Lambda_{\frac{1}{2\omega_2}}^{\omega_2}(r) = 2\,\Lambda_{\frac{1}{\omega_2}}(2r) - 2\,\omega_2\, r\,,$$

where $\Lambda_\lambda(r) = (r - s)/\lambda$, the value s being the real solution of the nonlinear equation $\lambda s^3 + s = r$, which has been solved for each r by using Cardano's formulae.

5.3. Numerical results: Comparison tests. In order to validate the correct performance of our numerical approach, we have considered a first test (Test 1), which presents a closed form stationary solution. It corresponds to a no sliding case (i.e., $u_b = 0$) and is adapted from Paterson [36]. More precisely, in Test 1, for a sufficiently large time interval $(0, T)$, we consider the open set $\Omega = (-L, L)$ and the following piecewise constant accumulation-ablation function:

$$a(x) = \begin{cases} a_1 & \text{if } 0 \le |x| < R, \\ -a_2 & \text{if } R \le |x| \le L, \end{cases} \tag{5.24}$$

where $L > 1$, $a_1 > 0$, $a_2 > 0$, and $R \in (0, 1)$. Moreover, we assume that

$$a_1 R = a_2(1 - R) \tag{5.25}$$

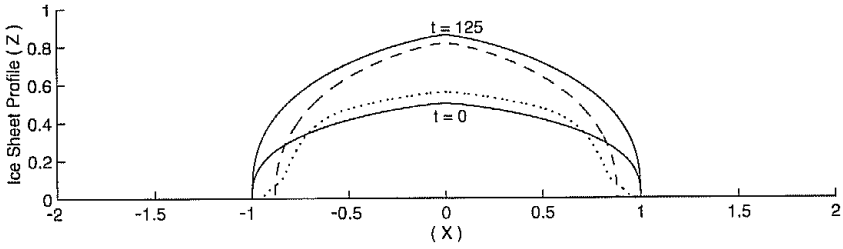

FIG. 5.1. *Computed numerical solution of Test* 1; $t = 0(-), t = 5(\cdots), t = 75(--)$, *stationary* $(-)$.

holds. Thus, for the particular values $a_1 = 0.01$ and $a_2 = 0.03$, we have the steady state solution

$$\overline{\eta}(x) = \begin{cases} H\left[1 - \left(1 + \dfrac{a_1}{a_2}\right)^{1/3} \left(\dfrac{|x|}{L}\right)^{4/3}\right]^{3/8} & \text{if } |x| \le R, \\ H\left(1 + \dfrac{a_2}{a_1}\right)^{1/8} \left(1 - \dfrac{|x|}{L}\right)^{1/2} & \text{if } R \le |x| \le 1, \\ 0 & \text{if } 1 \le |x| \le L, \end{cases} \tag{5.26}$$

where $H = (40\, a_1\, R)^{1/8}$ represents the thickness at $x = 0$ (the *ice divide*).

Moreover, in Test 1 the values $L = 2$ and $R = 0.75$ have been chosen so that $H = 0.86$. As initial conditions for the evolutive problem, we have considered

$$\eta_0(x) = \begin{cases} c\,(1 - |x|^{4/3})^{3/8} & \text{if } |x| \le 1, \\ 0 & \text{if } 1 \le |x| \le 2, \end{cases} \tag{5.27}$$

with $c = 0.5$.

For the numerical solution a uniform finite element mesh with $N = 4001$ nodes and a time step $\Delta t = 1$ have been taken.

In Figure 5.1 we present the initial profile ($t = 0$), the computed solutions for $t = 5$ and $t = 75$, and the stationary exact solution (which matches the numerical approximation for $t = 125$) for Test 1. Figure 5.1 is obtained with the described Bermúdez–Moreno method with $\omega_1 = 15$ and $\omega_2 = 30$. The computed results agree with the same test example solved with another numerical approach in Calvo, Durany, and Vázquez [13], but computing time is highly reduced (by about 99 per cent). Notice that in Figure 5.1 for $t = 5$ the ice sheet is retreating. The ice mass shrinks until $t = 25$, and then it expands with time until reaching the stationary solution given by expression (5.26). The initial contraction is mainly due to the fact that accumulation taking place at the center cannot balance the initial effect of ablation near the margins.

Test 2 is proposed to simulate the behavior of the concave profile when increasing the sliding velocity. In this case, we take $L = 2$ and $R = 1$ in (5.24), so that (5.25) is not verified. Thus, in Figures 5.2 and 5.3 several examples are presented by considering the velocity field

$$u_b(t,x) = \begin{cases} C\,x^2 & \text{if } x \ge 0, \\ -C\,x^2 & \text{if } x < 0 \end{cases} \tag{5.28}$$

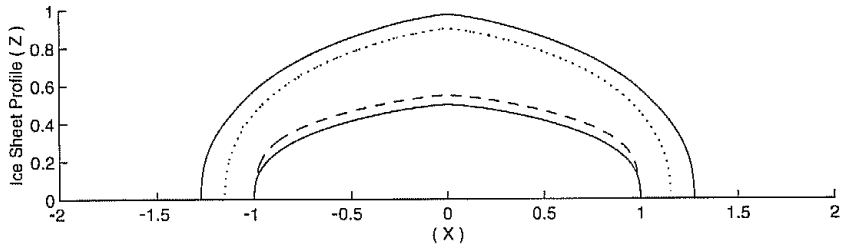

FIG. 5.2. *Numerical solution of Test 2 in the case* $C = 0.005$; $t = 0(-), t = 5(--)$, $t = 50(\cdots), t = 90(-)$.

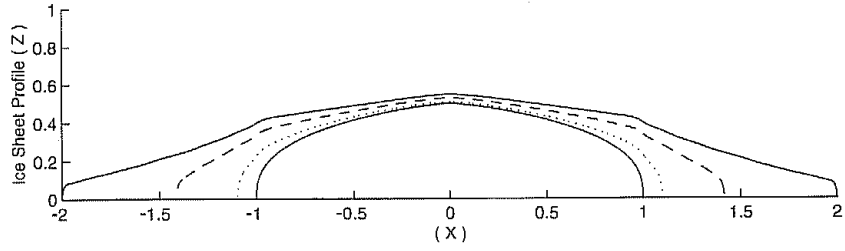

FIG. 5.3. *Numerical solution of Test 2 in the case* $C = 0.1$; $t = 0(-), t = 1(\cdots), t = 3(--), t = 5(-)$.

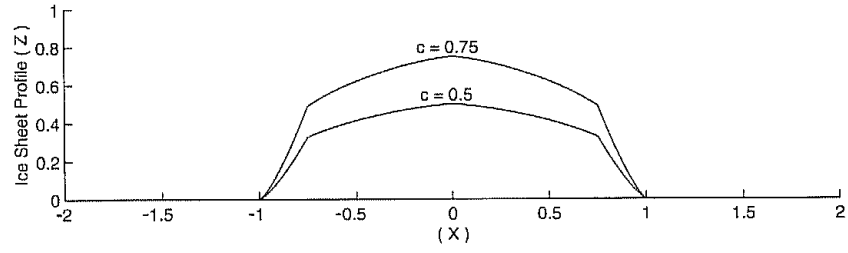

FIG. 5.4. *Convex-concave initial condition* $\overline{\eta}_0$ *for* $c = 0.5$ *and* $c = 0.75$.

and the initial condition (5.27). More precisely, Figure 5.2 shows the results obtained for $t = 5$, $t = 50$, and $t = 90$ in the case $C = 0.005$, and Figure 5.3 presents the computed profiles for $t = 1$, $t = 3$, and $t = 5$ when $C = 0.1$. These figures illustrate how concave profiles disappear in the presence of enough convection ($C = 0.1$). The values of time have been chosen to present the profiles that most emphasize this realistic phenomenon. The time step, the number of nodes, and the parameters in the Bermúdez–Moreno algorithm are the same as those used in Test 1.

Test 3 has been designed to illustrate the *waiting time property* discussed in section 4. The idea is to show how when the initial condition of the problem has a sufficiently flat convex-concave shape (see Figure 5.4), then the displacement of the initial free boundary ($S_+(t_0)$, for example) starts after a certain time (the *waiting time*). Nevertheless, an instantaneous displacement occurs for a concave initial condition (as (5.27), for example).

More precisely, in order to illustrate this so-called *waiting time property*, the numerical solutions obtained from the initial condition (5.27) and the following alter-

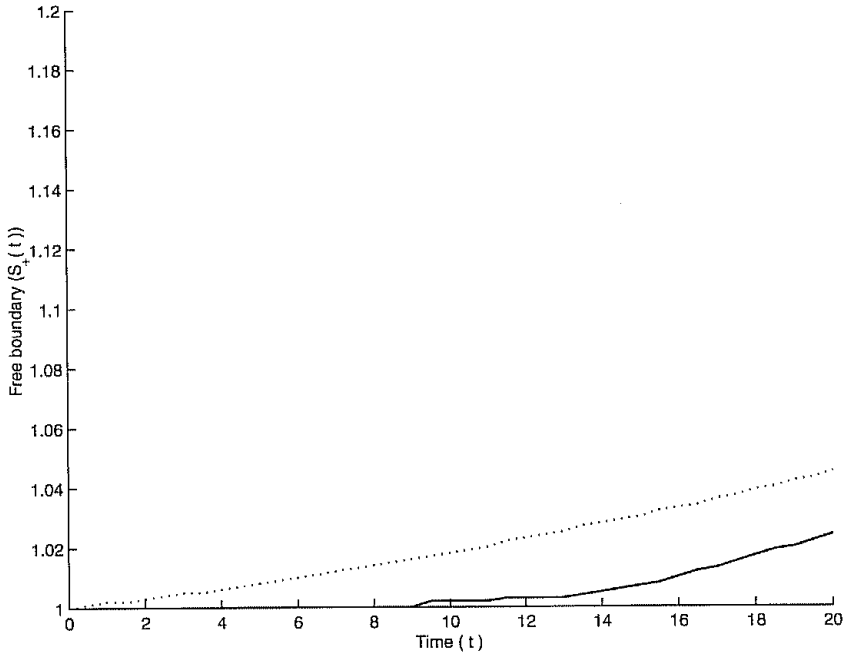

FIG. 5.5. *Moving boundary* $S_+(t)$ *in Test* 3, *with convex-concave* $\overline{\eta}_0$ $(-)$ *and purely concave* η_0 $(\cdots)$ *initial conditions for* $c = 0.5$.

native one,

$$\overline{\eta}_0(x) = \begin{cases} c\,(1-|x|^{4/3})^{3/8} & \text{if} \quad -0.75 \le x \le 0.75, \\ 16.77\,c\left(\dfrac{a_2}{2}\right)^{1/3} |x-1|^{4/3} & \text{if} \quad 0.75 \le x \le 1, \\ 16.77\,c\left(\dfrac{a_2}{2}\right)^{1/3} |x+1|^{4/3} & \text{if} \quad -1 \le x \le -0.75, \\ 0 & \text{otherwise}, \end{cases} \tag{5.29}$$

are compared for different values of c. Thus, in Figures 5.5 and 5.6 the moving boundaries are compared for the initial conditions (5.27) and (5.29) for $c = 0.5$ and $c = 0.75$, respectively. Notice that the theoretical result stated in section 4 about the *waiting time* property is a local one, while numerical observations yield a global *waiting time*. To our knowledge the proof of global *waiting time* properties is an open and difficult question.

Next we illustrate the relation between the *waiting time* and the initial ice mass stated in the theoretical analysis. As the ice mass associated with an initial condition such as (5.29) depends linearly on the parameter c, in Figure 5.7 we compare the moving boundary evolution for different values of c in the absence of convection. Notice how the *waiting time* decreases when the initial ice mass increases.

Finally, in Figure 5.8 the influence of convection for a fixed initial ice mass associated with $c = 0.75$ is illustrated. Thus, an increasing basal sliding reduces the *waiting time* as expected in real situations.

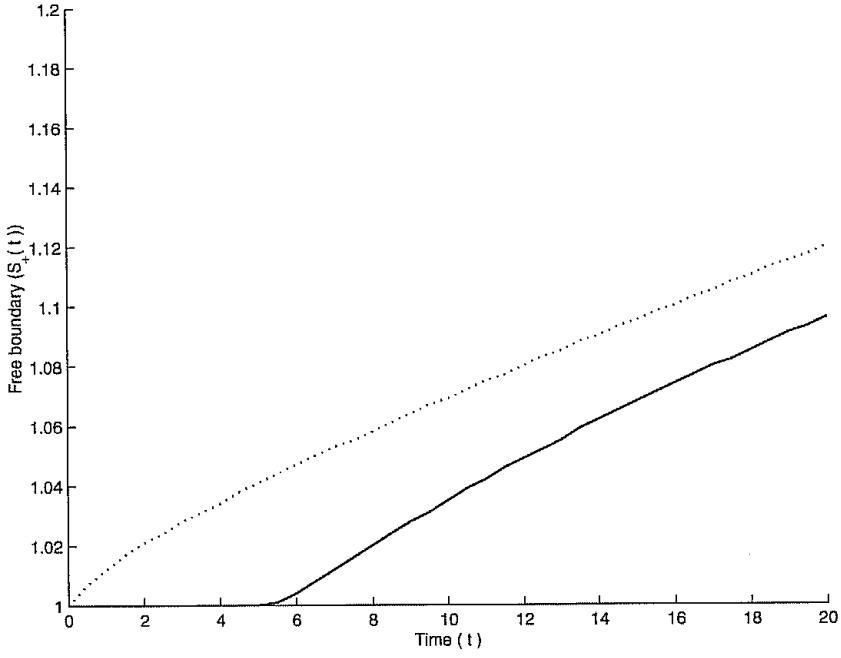

FIG. 5.6. *Moving boundary $S_+(t)$ in Test 3, with convex-concave $\overline{\eta}_0$ $(-)$ and purely concave η_0 $(\cdots)$ initial conditions for $c = 0.75$.*

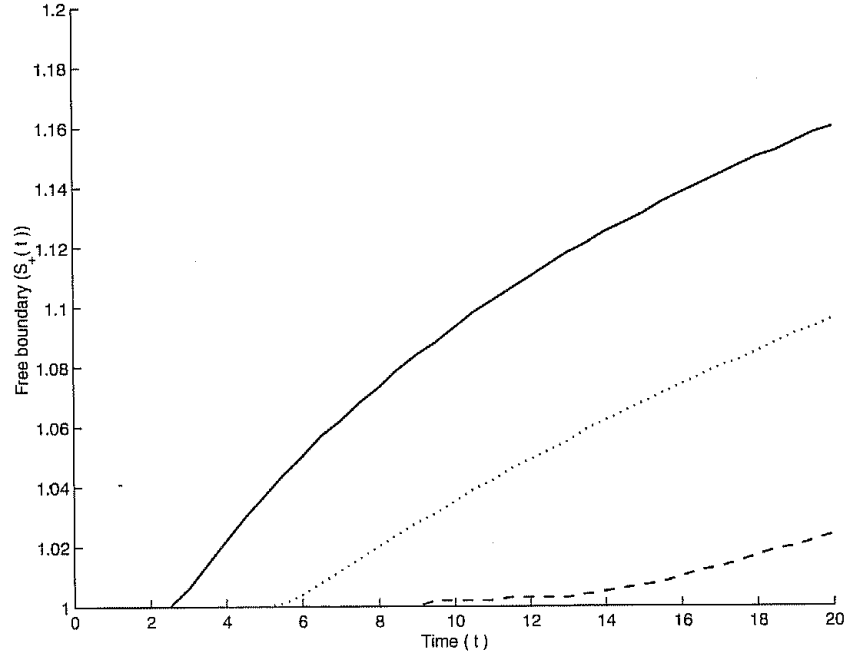

FIG. 5.7. *Moving boundary $S_+(t)$ in Test 3, with convex-concave $\overline{\eta}_0$ function and $C = 0$ for $c = 0.5(--), c = 0.75(\cdots), c = 0.9(-)$.*

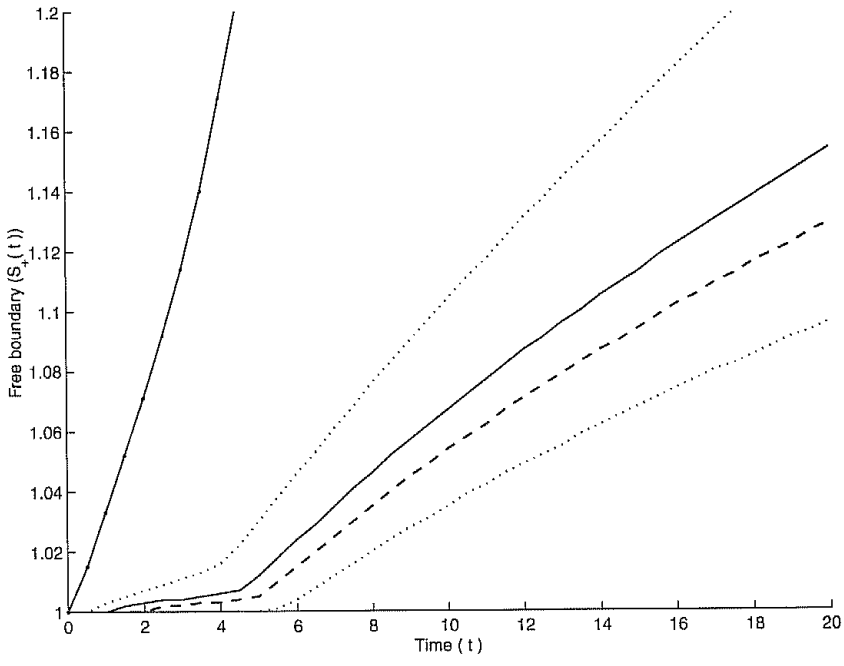

FIG. 5.8. *Moving boundary* $S_+(t)$ *in Test* 3, *with* $\overline{\eta}_0$ *and* $c = 0.75$; $C = 0(\cdots), C = 0.003(--), C = 0.005(-), C = 0.01(\cdots), C = 0.05(. - .-)$.

6. Discussion. In this paper we have used different but equivalent weak formulations, expressed in terms of either multivalued equations or variational inequalities when the complementarity formulation is considered for numerical purposes. This approach makes more precise the original doubly nonlinear formulation of Fowler [29], converting it into an obstacle problem for the associated operator. Assuming some extra regularity properties of the solution, we have given sufficient conditions (in terms of a, the accumulation rate, and h_0, the initial thickness) for the existence of the free moving boundary and its spatial location. For this, we employed two different methods: a comparison principle, combined with the construction of suitable barrier functions in the case $u_b \equiv 0$, and a local energy method if $u_b \neq 0$. In both cases, we prove rigorously the possible existence of a waiting time in the dynamics of the free boundary, whose location and evolution can be qualitatively described as long as suitable and physically admissible hypotheses on the data of the problem hold. From the numerical point of view, the main advantage of the proposed new approach follows from the introduction of a maximal monotone operator for the nonlinear diffusive term that had already been treated in explicit form [13]. Thus, a duality method can also be applied to greatly improve the speed of convergence with respect to the previous work. In order to verify the good performance of the new algorithm as well as the computational cost reduction, a problem with a closed form solution has been tested. Moreover, to complete the theoretical results and reflect some realistic situations, several test examples illustrate some qualitative properties of the ice profile and the associated free boundary.

REFERENCES

[1] S. N. Antontsev, J. I. Díaz, and S. I. Shmarev, *The support shrinking properties for solutions of quasilinear parabolic equations with strong absorption terms*, Ann. Fac. Sci. Toulouse Math., 4 (1995), pp. 5–30.

[2] S. N. Antontsev, J. I. Díaz, and S. I. Shmarev, *Energy Methods for Free Boundary Problems*, Birkäuser-Boston, Cambridge, MA, 2001.

[3] G. Bayada, M. Chambat and C. Vázquez, *Characteristics method for the formulation and computation of a free boundary cavitation problem*, J. Comput. Appl. Math., 98 (1998), pp. 191–212.

[4] Ph. Benilan and P. Wittbold, *On mild and weak solutions of elliptic-parabolic problems*, Adv. Differential Equations, 1 (1996), pp. 1053–1073.

[5] M. Bercovier, O. Pironneau, and V. Sastri, *Finite elements and characteristics for some parabolic-hyperbolic problems*, Appl. Math. Model., 7 (1983), pp. 89-96.

[6] R. Bermejo and J.-A. Infante, *A multigrid algorithm for the p-Laplacian*, SIAM J. Sci. Comput., 21 (2000), pp. 1774–1789.

[7] A. Bermúdez, *Un método numérico para la resolución de ecuaciones con varios términos no lineales. Aplicación a un problema de flujo de gas en un conducto*, Rev. R. Acad. Cienc. Exactas Fís. Nat. (Esp.), 78 (1981), pp. 485–495.

[8] A. Bermúdez and C. Moreno, *Duality methods for solving variational inequalities*, Comput. Math. Appl., 7 (1981), pp. 43–58.

[9] A. Bermúdez, M. C. Muñiz, and P. Quintela, *Numerical solution of a three-dimensional thermoelectric problem taking place in an aluminium electrolytic cell*, Comput. Methods Appl. Mech. Engrg., 106 (1993), pp. 129–142.

[10] L. Boccardo, D. Giachetti, J. I. Díaz, and F. Murat, *Existence of a solution for a weaker form of a nonlinear elliptic equation*, in Recent Advances in Nonlinear Elliptic and Parabolic Problems, Pitman Res. Notes Math. Ser. 208, Longman Scientific Technical, Harlow, UK, 1989, pp. 229–246.

[11] H. Brezis, *Opérateurs Maximaux Monotones et Semigroupes de Contractions dans les Espaces de Hilbert*, North–Holland, Amsterdam, 1973.

[12] N. Calvo, J. Durany, and C. Vázquez, *Numerical approach of temperature distribution in a free boundary polythermal ice sheet*, Numer. Math., 83 (1999), pp. 557–580.

[13] N. Calvo, J. Durany, and C. Vázquez, *Numerical computation of ice sheet profiles with free boundary problems*, Appl. Numer. Math., 35 (2000), pp. 111–128.

[14] N. Calvo, J. Durany, and C. Vázquez, *Numerical approach of thermomechanical coupled problems with moving boundaries in glaciology*, Math. Models Methods Appl. Sci., 12 (2002), pp. 229–249.

[15] J. Carrillo and P. Wittbold, *Uniqueness of renormalized solutions of degenerate elliptic-parabolic problems*, J. Differential Equations, 156 (1999), pp. 93–121.

[16] Z. Chen, R. H. Nochetto, and A. Schmidt, *A characteristics Galerkin method with adaptive error control for the continuous casting problem*, Comput. Methods Appl. Mech. Engrg., 189 (2000), pp. 249-276.

[17] J.I. Díaz, *Elliptic and parabolic quasilinear equations giving rise to a free boundary: The boundary of the support of the solution*, in Nonlinear Functional Analysis and Applications, F. E. Browder, ed., Proc. Sympos. Pure Math. 45.2, AMS, Providence, RI, 1986, pp. 381–393.

[18] J. I. Díaz and F. de Thelin, *On a nonlinear parabolic problem arising in some models related to turbulent flows*, SIAM J. Math. Anal., 25 (1994), pp. 1085–1111.

[19] J. I. Díaz and G. Galiano, *On the Boussinesq system with nonlinear thermal diffusion*, Nonlinear Anal., 30 (1997), pp. 3255–3263.

[20] J. I. Díaz and J. Hernández, *Qualitative properties of free boundaries for some non linear degenerate parabolic equations*, in Nonlinear Parabolic Equations: Qualitative Properties of Solutions, L. Boccardo and A. Tesei, eds., Pitman Res. Notes Math. Ser. 149, Longman Scientific and Technical, London, 1989, pp. 85–93.

[21] J. I. Díaz and E. Schiavi, *Tratamiento matemático de una ecuación parabólica cuasilineal degenerada en Glaciología*, in Electronic Proceedings of the XIV CEDYA-IV Congreso de Matemática Aplicada, Vic, Barcelona, 1995, http://www.mal.upc.es/cedya/cedya.html.

[22] J. I. Díaz and E. Schiavi, *On a degenerate parabolic/hyperbolic system in glaciology giving rise to a free boundary*, Nonlinear Anal., 38 (1999), pp. 649–673.

[23] J. I. Díaz and L. Veron, *Local vanishing properties of solutions to elliptic and parabolic equations*, Trans. Amer. Math. Soc., 290 (1985), pp. 787–814.

[24] R. J. Di Perna and P. L. Lions, *On the Cauchy problem for Boltzmann equations: Global existence and weak stability*, Ann. of Math., 130 (1989), pp. 321–366.

[25] J. DURANY, G. GARCÍA, AND C. VÁZQUEZ, *An elastohydrodynamic coupled problem between a piezoviscous equation and a hinged plate model*, M2AN Math. Model. Numer. Anal., 31 (1997), pp. 495–516.

[26] J. DURANY, G. GARCÍA, AND C. VÁZQUEZ, *Numerical simulation of a lubricated Hertzian contact problem under imposed load*, Finite Elem. Anal. Des., 38 (2002), pp. 645–658.

[27] G. DUVAUT AND J. L. LIONS, *Les inéquations en Mécanique et en Physique*, Dunod, Paris, 1972.

[28] L. C. EVANS AND B. F. KNERR, *Instantaneous shrinking of the support of nonnegative solutions to certain nonlinear parabolic equations and variational inequalities*, Illinois J. Math., 23 (1979), pp. 153–166.

[29] A. C. FOWLER, *Modelling ice sheet dynamics*, Geophys. Astrophys. Fluid Dyn., 63 (1992), pp. 29–65.

[30] A. C. FOWLER, *Mathematical Models in the Applied Sciences*, Cambridge University Press, Cambridge, UK, 1997.

[31] A. C. FOWLER AND E. SCHIAVI, *A theory of ice-sheet surges*, J. Glaciology, 44 (1998), pp. 104–118.

[32] K. HUTTER, *Theoretical Glaciology*, Reidel, Dordrecht, The Netherlands, 1981.

[33] L. LLIBOUTRY, *Very Slow Flows of Solids*, Martinus Nijhoff, Dordrecht, The Netherlands, 1987.

[34] R. H. NOCHETTO, *Numerical methods for free boundary problems*, in Free Boundary Problems: Theory and Applications, K.H. Hoffman and J. Sprekels, eds., Pitman Res. Notes Math. Ser. 185–186, Longman Scientific and Technical, London, 1990, pp. 555–566.

[35] R. H. NOCHETTO AND C. VERDI, *Approximation of degenerate parabolic problems using numerical integration*, SIAM J. Numer. Anal., 25 (1988), pp. 784–814.

[36] W. S. B. PATERSON, *The Physics of Glaciers*, Pergamon, Oxford, 1981.

[37] O. PIRONNEAU, *On the transport-diffusion algorithm and its application to Navier-Stokes equation*, Numer. Math., 38 (1982), pp. 309–332.

[38] L. TARASOV AND W. R. PELTIER, *Terminating the 100 kyr ice age cycle*, J. Geophys. Res., 102 (1997), pp. 21665–21693.